FOURIER MASK OPTICS

Thesis for the Degree of M. S.

MICHIGAN STATE UNIVERSITY

John Frederick Kelsey

1965

ABSTRACT

FOURIER MASK OPTICS

by John Frederick Kelsey

The Foucault knife edge test, the schlieren system, the phase contrast method, and the concepts of spatial filtering and theta modulation are all characterized by the same mathematical expressions. These concepts are grouped here under the title "Fourier Mask Optics" where the word mask includes phase masks as well as the usual sense, i.e., amplitude masks. A general mathematical procedure is derived from basic principles and the manner in which the aforementioned concepts fit into this mathematical framework is shown by way of a simple example of each case. Several illustrations of interesting subjects are also shown, with emphasis on the schlieren system and the special case of isochromates.

FOURIER MASK OPTICS

By

John Frederick Kelsey

A THESIS

Submitted to
Michigan State University
in partial fulfillment of the requirements
for the degree of

MASTER OF SCIENCE

Department of Physics and Astronomy

1965

ACKNOWLEDGEMENTS

I would like to thank Professor E. A. Hiedemann for his guidance and helpful suggestions. Thanks are also due Dr. B. D. Cook, Dr. Y. F. Bow, Dr. W. R. Klein, Dr. W. G. Mayer, and the entire Ultrasonics Group for their aid, encouragement and helpful criticism.

J. F. K.

Table of Contents

List of Figures

INTRODUCTION

There are several optical systems which are characterized by the fact that somewhere between the object and its image a distribution of light is formed similar to the Fourier transform of the light distribution leaving the object. By masking this Fourier pattern almost any information from the object can be selectively removed or passed to the image.

Examples of Fourier mask optical systems are the following: the Foucault knife edge test; the schlieren system; the phase contrast method and the concepts of spatial filtering and theta modulation. It should be noted that the word mask as used here includes phase masks as well as the usual sense, i. e., amplitude masks.

For a qualitative understanding of Fourier mask optics consider the idealized null schlieren system shown in Fig. 1d and the conceptual steps (Fig. 1a, b, c) in assembling the system.

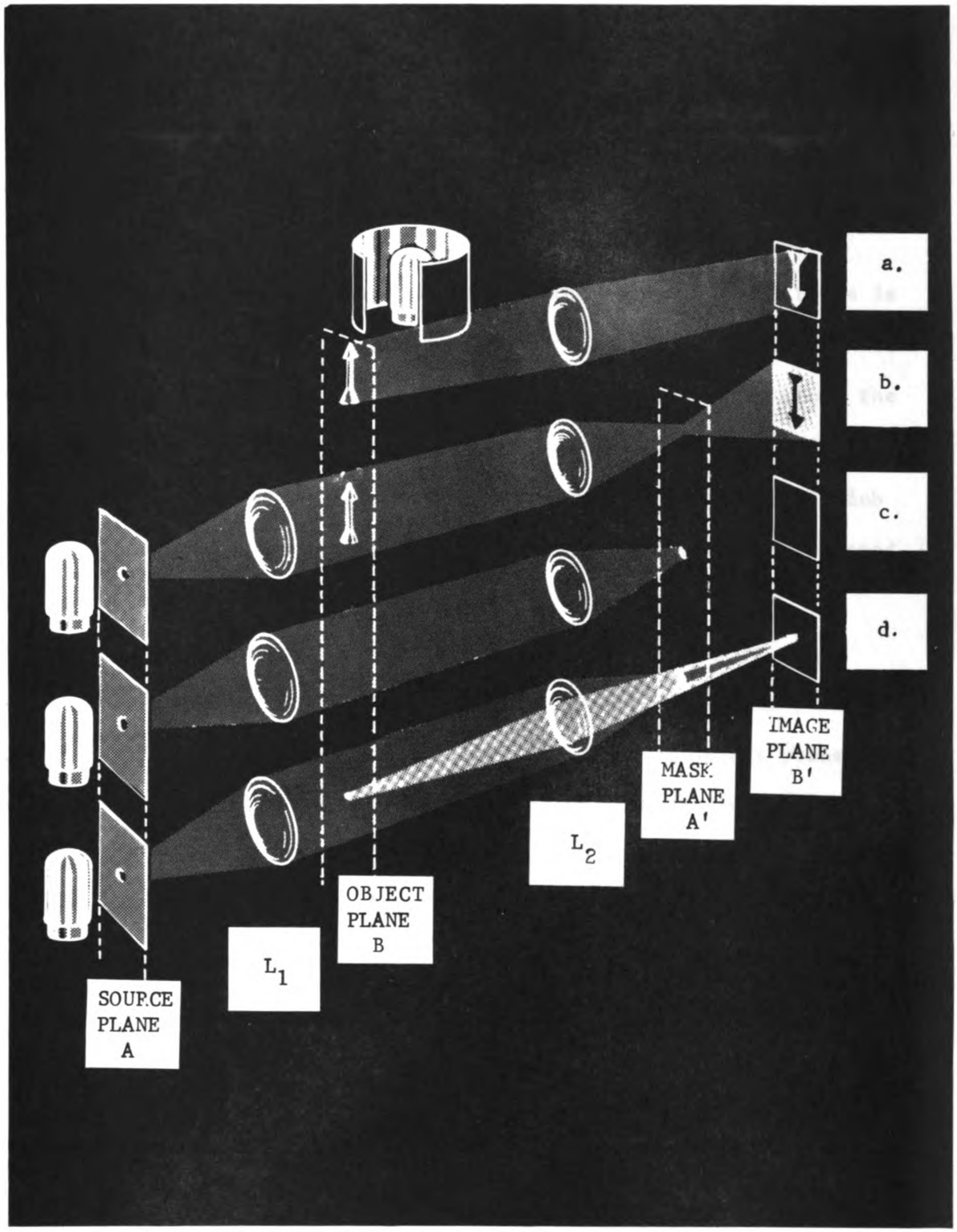

Fig. 1. The conceptual steps in assembling a Fourier Mask System

Part (a) of Fig. 1 will be recognized as a simple camera. An arrow in the object plane B is illuminated by the light at the top of the figure. An image of the arrow is formed by the lens L_2 in the image plane B'. In part (b) the object is illuminated by collimated light from a small axial source. The arrow is now imaged in silhouette at B' and there is an image of the point source in the plane A'. In the next step the arrow is removed and a mask is placed in the mask plane A' so as to block the image of the point source. Since no light passes A' the image plane B' will be in darkness. Now, if an object is placed in the B plane which deflects the light sufficiently to miss the mask then it will be imaged on the B' plane by lens L_2.

It will be shown later that in the approximation of ideal optical components the light distribution approaching the mask plane A' is just the Fourier transform of the light leaving the object plane B, and in turn the light distribution of the image at B' is just the Fourier transform of the light distribution leaving the mask plane A'. A distinction must be made between the light distribution approaching and leaving the mask plane A' since a difference is introduced due to the presence of the mask. The mask will be characterized by a mask function M such that M operating on the light distribution E approaching the mask plane A' yields the light distribution $E' = ME$ leaving the mask plane A'.

The mathematical procedure used to determine the light distribution in the final image is as follows:

1. The Fourier transform of the light distribution leaving the object gives the light distribution approaching the mask plane A'.

2. The light distribution approaching the mask plane is multiplied by the mask function M yielding the light distribution leaving the mask plane A'.

3. The Fourier transform of the light leaving the mask plane yields the light distribution of the final image at the plane B'.

In order to understand the limitations of the procedure outlined above the Fourier transform properties of a lens will be derived from Huygen's principle in Chapter II. In Chapter III a general treatment of objects is given along with the resulting light distribution approaching the mask plane. Before proceeding to the final two steps outlined above, i.e., the effect of mask and the final image, Chapter IV is introduced to discuss various source configurations in the plane A. Chapter V begins with a general discussion of the effect of mask and the final image, and concludes with a treatment and illustrations of those Fourier mask optical systems which have become most useful.

II. THE FOURIER TRANSFORM PROPERTY OF A LENS

The following is a derivation of optical image formation similar to that first given by Porter[1]. Let us begin by examining the situation between the lens L_2 and the mask plane A'. (see Fig. 1). Consider the space description of a perfectly spherical wavefront of light formed by the lens L_2 and converging toward the origin of the plane A'. The amplitude of the electric vector may be written as

$$E_B = E_R \exp [-ikR], \tag{1}$$

where E_R is the electric field at R, k is the optical wave constant, and R is the radius of the spherical surface as shown in Fig. 2.

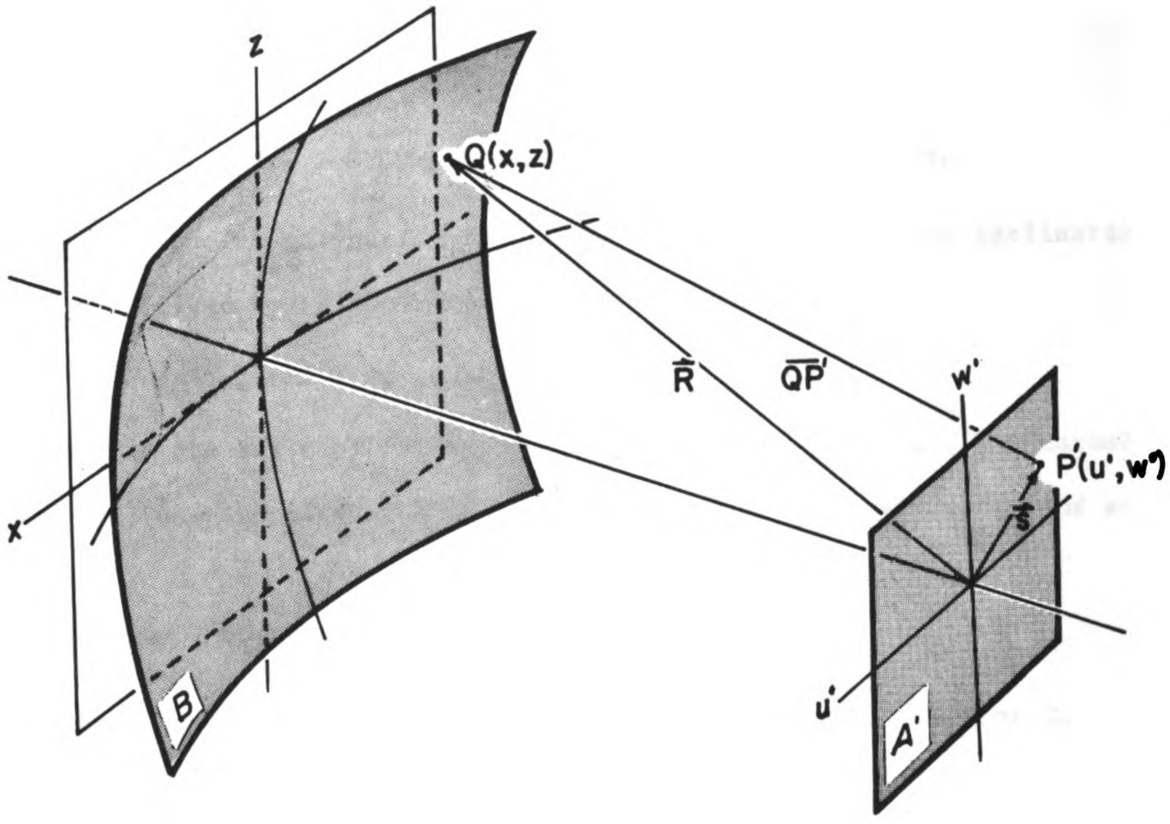

Fig. 2. A spherical wavefront concentric about the origin of the Mask Plane.

The coordinates u', w' describe points on the plane A' and the coordinates x, y, z describe points on the spherical surface B. The equivalence of this spherical surface B and the object plane B mentioned in the introduction depends on the intervening lens L_2 and will be discussed later in this chapter.

The optical disturbance at an arbitrary point P'(u',w') near the origin can be calculated by applying Huygen's principle, i.e., by considering each element of the spherical surface B as a secondary source, and summing the contributions from all of these secondary sources at the point P'(u',w'). Let Q(x,z) be an arbitrary point on the spherical surface B, the disturbance at P'(u',w') due to a point source at Q(x,z) is then given by

$$dE(u',w') = C\, K(\alpha)\, E_R \exp[-ikR]\, \frac{\exp[ik\overline{QP'}]}{\overline{QP'}}\, dx\, dz, \tag{2}$$

where C is the normalization factor and $K(\alpha)$ is the familiar inclination factor[2] given by

$$K(\alpha) = -\frac{ik}{2\pi}(1 + \cos\alpha), \tag{3}$$

where α is the angle of diffraction, i.e., the angle between the normal at Q(x,z) and the direction $\overline{QP'}$. In this case α is always small and so one has

$$K(\alpha) \approx -\frac{ik}{\pi}. \tag{4}$$

Now, by including the constant $-ik/\pi$ in the normalization factor C, Eq. (2) can be written

$$dE(u',w') = C\, E_R \exp[-ikR]\, \frac{\exp[ik\overline{QP'}]}{\overline{QP'}}\, dx\, dz. \tag{5}$$

The disturbance at P'(u',w') due to the entire surface B is just

$$E(u',w') = C\iint_B E_R \exp[-ikR] \frac{\exp[ik\overline{QP}']}{\overline{QP}'} dx\, dz. \tag{6}$$

Considering the vectors $\overline{R}$ and $\overline{s}$ as shown in Fig. 2 the distance $\overline{QP}'$ can be written as

$$\overline{QP}'^2 = R^2 + s^2 - 2\overline{R}\cdot\overline{s}. \tag{7}$$

Since $\overline{s}$ is much smaller than $\overline{R}$ the distance $\overline{QP}'$ may be approximated by

$$\overline{QP}' \approx R - \frac{1}{R}(u'x + w'z). \tag{8}$$

With these approximations Eq. (6) becomes

$$E(u',w') = \frac{C}{R}\iint_B E_R \exp[-\frac{ik}{R}(u'x + w'z)]\, dx\, dz. \tag{9}$$

If the light distribution is not uniform over the surface B, then E_R will be a function of x and z and must be left inside the integral. In general E_R will be a complex function which will be written as E(x,z). Using this notation Eq. (9) now becomes

$$E(u',w') = \frac{C}{R}\iint_B E(x,z) \exp[-\frac{ik}{R}(u'x + w'z)]\, dx\, dz. \tag{10}$$

From Eq. (10) it can be seen that the light distribution approaching the mask plane A' is just the Fourier transform of the light distribution on a spherical surface at a distance R very large compared to u' and w'.

Equation (10) is the basic expression of the Fourier transform property of a lens and will be used extensively later.

A similar derivation shows that the Fourier transform of the light distribution E'(u'w') leaving the mask plane A' gives the light

distribution in the image plane B' as

$$E(x',z') = \frac{C}{R_2}\iint_{A'} E'(u',w') \exp\left[-\frac{ik}{R_2}(x'u' + z'w')\right] du'\, dw', \quad (11)$$

where R_2 is the distance from the mask plane A' to the image plane B'.

Equations (10) and (11) along with the expression,

$$E'(u',w') = M(u',w')\, E(u',w'). \quad (12)$$

constitute a set of equations giving the final image $E(x',z')$ for a given mask function and object, provided we can prove the equivalence of the object plane B and the spherical surface B.

It can be shown from the Eikonal equation[3] that the spherical surface and the object plane are equivalent under certain restrictions.

To investigate these restrictions consider the light distribution approaching the mask plane A' due to a perfect lens L_2 with a circular aperture. The light on the spherical surface B is limited to a region $x^2 + z^2 < h^2$. Making the transformation to polar coordinates defined by

$$r\cos\theta = x, \qquad r\sin\theta = z,$$

$$s\cos\theta' = u', \text{ and} \qquad s\sin\theta' = w', \quad (13)$$

gives

$$u'x + w'z = rs\cos(\theta - \theta'). \quad (14)$$

Due to the circular symmetry of the problem, no generality is lost by setting $\theta' = 0$. The light distribution at the mask plane, given by Eq. (10), for this case is

$$E(s,\theta') = \frac{C}{R}\int_0^h\int_0^{2\pi} E(r,\theta) \exp\left[-\frac{ik}{R} rs\cos\theta\right] r\,d\theta\,dr. \quad (15)$$

The integration over r has been taken only from the origin to the margin h of the spherical surface, because the value of $E(r,\theta)$ outside the limits of integration is zero. Assuming uniform illumination, $E(r,\theta)$ can be taken as a constant in the region $r < h$ and can be taken outside the integral.

Using an integral representation for the Bessel functions[4],

$$J_n(S) = \frac{i^{-n}}{2\pi}\int_0^{2\pi} \exp\,[i(na + S\cos a)]\,da, \tag{16}$$

Eq. (15) may be written

$$E(s,\theta') = C'\int_0^h J_o\left(\frac{ks}{R}\,r\right) r\,dr. \tag{17}$$

After integration and normalization, Eq. (17) becomes

$$E\,(s,\theta') = \frac{J_1\left(\frac{kh}{R}\,s\right)}{\frac{kh}{R}\,s}\,, \tag{18}$$

which is the well known expression for the amplitude of the Airy pattern. Noting that the first zero of J_1 occurs when the argument khs/R equals 3.83, we have the familiar equation for the diameter of the central disk

$$2s = \frac{1.22\lambda}{h/R}\,. \tag{19}$$

It is important to note from Eq. (19) that for a given wavelength the Airy pattern does not depend on the distance R alone but rather on the angle $\tan^{-1}(h/R)$. This, in essence, states that any spherical surface subtending the same angle produces an identical Airy pattern. For the case in point we choose the surface with R equal to f, the focal length of the lens L_2.

The Eikonal equation goes even further than Eq. (19) to state that the light distribution on any wavefront of an optical system can be used for these calculations, provided there are no intervening obstacles. With this in mind the restrictions governing the equivalence of the object plane B and the spherical surface B can be immediately written down as follows:

1. The lens L_2 must be of sufficient aperature so as not to constitute an obstacle.

2. The lens must be good enough to convert a plane wavefront into a spherical wavefront.

It should be noted that for an object that diffracts light at large angles, the first restriction limits the distance from the object to the lens and the proximity of the object to a marginal ray. This condition is exactly the resolving condition, so restriction 1 may be restated as:

1. The lens must be able to resolve the object. This restriction is self evident and merits no further mention.

The second restriction, on the other hand, is very difficult to meet rigorously, even with quality optics. This should not be surprising since the Foucalt knife edge test and the first schlieren systems were originally developed to examine minute deviations from geometrical perfection in optical components. The extent to which this geometrical restriction may be relaxed depends on the desired sensitivity of the Fourier mask system. For many objects the sensitivity need not be too

high. Nonetheless, insufficient lens or mirror quality is still the horror of precision Fourier mask methods. Since, however, the problem of lens quality at most is one of finance, we shall proceed idealistically by treating only the case of a geometrically perfect optics.

With these limitations in mind the light distribution approaching the mask plane A' shall henceforth be assumed to be exactly the Fourier transform of the light in the object plane B and no further mention of the resolving power of the lens L_2 or the geometrical quality of the optical system will be made.

III. OBJECT FUNCTIONS AND THEIR FOURIER TRANSFORMS

As outlined earlier, the first step in determining the final image from a Fourier mask system is to write an expression for the light distribution leaving the object, and to take its Fourier transform determining the light distribution approaching the mask plane A'.

Objects in general will introduce both phase and amplitude variations. The light distribution leaving the object can, in general, be written

$$E(x,z) = G(x,z) \exp [iH(x,z)] \tag{20}$$

Following the usual convention this expression will be called the object function. The amplitude factor $G(x,z)$ and the phase factor $H(x,z)$ are independent and may be expanded separately. Amplitude and phase factors of interest usually fall into two categories: those varying slowly which can best be expanded in power series; and those varying rapidly and showing periodicity which are best expanded in Fourier series. Other objects which are neither periodic nor smooth can still be treated using the fortunate characteristic, that the Fourier transform is an integral or addition process. This allows the expression of different parts of the object in whichever expansion is best fitted and then summing the integrals. The integral limits take care of discontinuities.

With this in mind, the four cases which will be treated in some detail for the one dimensional case, are the following:

$$\begin{aligned} &\text{A.}\quad G(x) = \sum_n a_n x^n \ ; \\ &\text{B.}\quad H(x) = \sum_n b_n x^n \ ; \\ &\text{C.}\quad G(x) = \sum_n a_n \sin(nk^*x + \phi_n) \ ; \\ &\text{D.}\quad H(k) = \sum_n V_n \sin(nk^*x + \phi_n) \ . \end{aligned} \tag{21}$$

These are sufficient to handle any object function.

A. Pure Amplitude Object, Power Series.

In practice, this case is not of much interest, so only the linear case will be treated. The light distribution approaching the mask plane given by the Eq. (10) becomes

$$E(u') = \frac{c'}{f} \int_{-h}^{h} x \exp[-\frac{ik}{f}(u'x)]\, dx. \tag{22}$$

The solution is

$$E(u') = 2i\, h^2 \ \frac{C'}{f} \left[\frac{\cos \frac{kh}{f} u'}{\frac{Kh}{f} u'} - \frac{\sin \frac{kh}{f} u'}{(\frac{kh}{f} u')^2} \right]. \tag{23}$$

It is interesting to note that E(u') at u' = 0 is finite, even though each term in the bracket is infinite. Furthermore, the intensity approaching the mask plane is symetric about u' = 0 even for the case of the density wedge.

B. Pure Phase Object, Power Series

First consider the case where the phase factor H(x,z) is a linear function of x. The amplitude function is a constant so Eq. (10)

can be written

$$E(u') = \frac{c}{f}\int_{-h}^{h} \exp\left[-ix\left(\frac{ku'}{f} - b_1\right)\right] d_x. \tag{24}$$

This is just the Airy pattern again with a displacement of the origin to u' equal to fb_1/k as would be expected from inserting a glass wedge. The next term in the series x^2 is exactly the problem encountered when examining thermal gradients[5]. Also, by examining small amounts of wave front curvature introduced by the x^2 term the light distribution just in front of and just behind the focal plane can be determined [6].

C. Pure Amplitude Object, Fourier Series

Consider the case of a pure amplitude object of the form

$$G(x) = \sum_n a_n \cos\left(nk^*x + \phi_n\right), \tag{25}$$

where k* is the wave constant of the basic periodicity of the object. In the more recent literature, the quantity $k^*/2\pi = 1/\lambda^*$ is called the spatial frequency. For this case Eq. (10) becomes

$$E(u') = \frac{C}{f} \sum_{n=-\infty}^{\infty} a'_n \exp\left[i\phi_n\right]\int_{-h}^{h} \exp\left[-ix\left(\frac{ku'}{f} + nk^*\right)\right] dx. \tag{26}$$

For large h this expression approaches the Dirac delta function at the values $nk^* = ku'/f$. This condition can be more easily recognized in terms of λ as

$$\frac{\lambda}{\lambda^*} = n\,\frac{u'}{f} \tag{27}$$

which will be recognized as the grating equation. From Eqs. (26) and (27) it is apparent that there will exist a set of discrete lines whose

intensity are given by

$$I_n = \frac{C^2}{f^2} \quad a_n^2 \tag{28}$$

So it can be seen that a lens truly Fourier analyzes the spatial frequencies of a pure amplitude object illuminated with coherent light. It is the masking of this spatial frequency spectrum that is the basis of the concept of spatial filtering[7,8].

D. Pure Phase Object, Fourier Series.

The case of an arbitrary phase object gives rise to a light distribution in the mask plane of the form

$$E(u') = \frac{C}{f}\int_{-h}^{h} \exp[\sum_n V_n \sin(nk^*x + \phi_n) + ikx]\, dx. \tag{29}$$

This integral has been solved explicitly[9]. The light amplitude in the nth diffraction order for large h is given by

$$E_m(u') = \sum_{k_2} \sum_{k_3} \cdots \sum_{k_\infty=-\infty}^{\infty} J_{m-2k_2-3k_3\cdots}(V_1)\, J_{k_2}(V_2)$$

$$J_{k_3}(V_3)\cdots \exp[-i(k_2\phi_2 + k_3\phi_3 + \cdots)]. \tag{30}$$

This expression is difficult to evaluate except for cases where higher harmonics are present only in small amounts. This case has received considerable attention because to certain approximations it characterizes the optical effect produced by an ultrasonic wave showing finite amplitude distortion.

In the section dealing with isochromates we shall have occasion to treat the case of a pure sinusoidal ultrasonic wave. For this case Eq. (30) reduces to

$$E_m(u') = J_m(V_1) \ . \tag{31}$$

This result was first given by Raman and Nath[10]. From Eq. (31) it can be seen that phase objects are <u>not</u> simply frequency analyzed in the mask plane, rather a single spatial frequency phase object gives rise to many diffraction orders. Great care must be taken to eliminate phase irregularities over the object if one wishes to use an optical system as a frequency analyzer.

IV. ILLUMINATION OF THE OBJECT

In Chapter III enough examples were worked so that the light distribution approaching the mask plane can now be determined for most objects of interest. Before proceeding to the effects of masks (Chapter V), mention should be made of how to treat source configurations in the plane A other than the point source which has been used exclusively until now.

If a second point source were added in the source plane A, there would be two Fourier patterns in the mask plane A'. These Fourier patterns which we called E(u',w') in Chapter III were developed assuming a single point source illumination. The function E(u',w') developed in this way is usually referred to as the spread function. For the remainder of this section we will call the spread function S(u',w') and reserve E(u',w') for the sum of the spread functions from various point sources.

If the two point sources mentioned above are coherent, the electric vectors of the spread functions will add in any region of overlap. If the two point sources have no fixed phase relationship, then the intensity of the spread functions will add in the mask plane.

For simplicity we take unit magnification between the source and mask plane, then we may write the preceding statements as

$$E(u',w') = \iint_A E(-u,-w)\ \ S(u' + u,\ w' + w)\ dA, \tag{32}$$

for the coherent case, and

$$I(u'w') = \iint_A I(-u,-w)\ \left|S(u' + u,\ w' + w)\right|^2\ dA, \tag{33}$$

for the incoherent case, where E(-u,-w) and I(-u,-w) represent the source configuration in the plane A. These are the general expressions needed to determine the light distribution approaching the mask plane for any source and object.

Later some qualitative mention will be made of how different source-mask pairs affect the resolution and speed of various Fourier mask systems, but all theoretical treatment will be for the simple case of a single point source. For this case E(-u,-w) is a delta function at u = w = 0 and Eq. (32) becomes

$$E(u'w') = S(u',w'), \tag{34}$$

which was our original convention.

V. THE MASK FUNCTION AND FINAL IMAGE

As was outlined earlier the mask function M(u',w') multiplied by the light distribution E(u',w') approaching the mask plane yields the light distribution E'(u',w') leaving the mask plane. The final image in the plane B', is just the Fourier transform of E'(u',w') as shown by

$$E(x',z') = \frac{C}{R_2}\iint_{A'} M(u',w')\ E(u'w')\ \exp[-\frac{ik}{R_2}\ (u'x'+w'z')]du'dw'. \qquad (35)$$

Equation (35) can be written more compactly in terms of the Fourier transforms of M(u',w') and E(u',w'). Utilizing convolution theory, Eq. (35) becomes

$$E(x',z') = \iint_{B} E(x,z)\ N(\frac{x'}{R_2} + \frac{k}{f}\ ,\ \frac{z'}{R_2} + \frac{z}{f})\ dxdz, \qquad (36)$$

where N is the Fourier transform of M(u',w'). This form has the advantage that we need not take the Fourier transform of the object function E(x,z), but we now must take the Fourier transform of the mask function M(u',w'). This in general is easier to do since mask functions are usually constants over various regions of A'.

Despite the mathematical simplicity of Eq. (36) it is difficult to follow the physical significance of the effect of masks on various information from the objects. We, therefore, shall return to the somewhat more complicated Eq. (35). In this form it is easy to understand the effect of mask on information from an object, because the object function can be written in two parts: one part that is affected by the mask, and one part that is not. Since this will be the general procedure followed

it is worthwhile to begin by considering the case of no mask at all before proceeding to specific Fourier mask systems. With no mask present $E'(u',w') = E(u',w')$ so the final image, given by Eq. (11), becomes

$$E(x',z') = \frac{C}{R_2}\iint_{A'} E(u',w') \exp\left[-\frac{ik}{R_2}(u'x' + w'z')\right] du'dw'. \tag{37}$$

The inverse Fourier transform of $E(u',w')$ is

$$E(x,z) = \frac{C}{f}\iint_{A'} E(u',w') \exp\left[\frac{ik}{f}(u'x + w'z)\right] du'dw'. \tag{38}$$

By redefining the coordinate system of the image plane as

$$x' = -\frac{R}{f}x \qquad \text{and} \qquad z' = -\frac{R}{f}z \tag{39}$$

Eqs. (37) and (38) yield

$$f\,E(x',z') = R_2\,E(x,z)\ . \tag{40}$$

This is the result expected for no mask, that is, neglecting the brightness, the image is just the object inverted and magnified. With the redefined coordinates x', z' the object and its image will be identical functions of x, z and x', z' respectively.

We now have the mathematical procedure to handle those special types of Fourier mask systems which have developed into systems of practical importance. We will begin by briefly treating the case of spatial filtering and simple phase contrast, and finish the chapter with a treatment of three special types of schlieren systems. The first, for viewing very feeble phase objects, is a null schlieren system. The second, for making quantitative measurements, is a schlieren interferometer. The third,

for viewing ultrasonic beam patterns, is the isochromate method.

A. Spatial Filtering

It was shown earlier that a pure amplitude grating is exactly frequency analyzed in the mask plane. The expression for the spatial frequency distribution in the mask plane, given by Eq. (27), can be rewritten as a vector equation and is given by

$$\overline{k^*}/2\pi = \pm\, \overline{ks}/2\pi f \tag{41}$$

From Eq. (41) it is obvious that a circular obstacle of radius b in the center of the mask plane is a high pass filter, blocking all spatial frequencies $k^*/2\pi < kb/2\pi f$. Also a circular aperature is a low pass filter and an annular aperature is a band pass filter. By observing the filtered image one can see just which spatial frequencies go into making up the object.

As an example of spatial filtering Fig. 3 shows the optical analogy of the common electronic practice of using a square wave input to test "time frequency" response. The photographs on the right are the spectra of frequencies that are allowed to pass, i.e., frequencies that are not blocked out by the mask, and the resulting image is on the left. It is possible to see in Fig. 3 the spatial frequency composition of an amplitude object.

The presence of small amounts of the even harmonics is due to the fact that the Ronchi ruling used introduced phase irregularities through the transparent parts of the ruling.

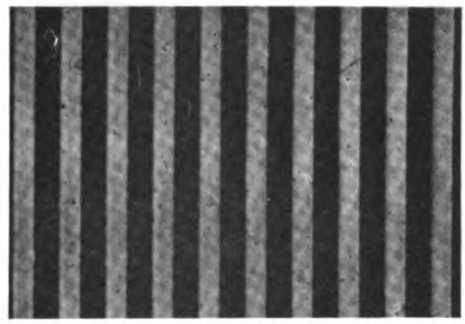

all frequencies

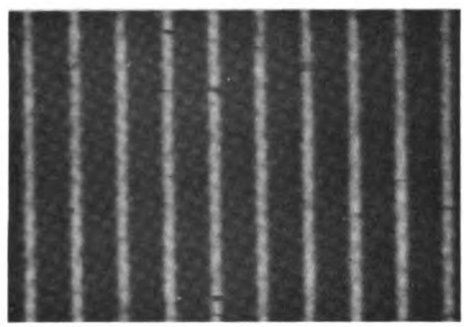

0th and 1st orders

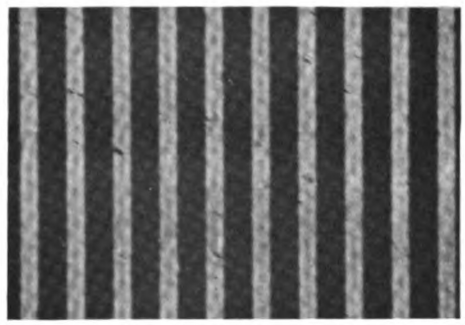

0th, 1st, and 3rd orders

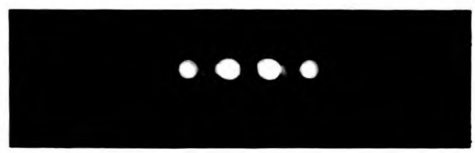

1st, 3rd, and 5th orders

Fig. 3. The spatial frequency composition of a square wave amplitude object


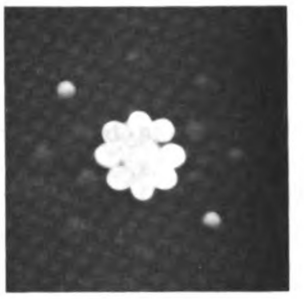

all


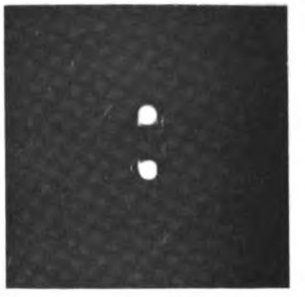

No. 1 0°


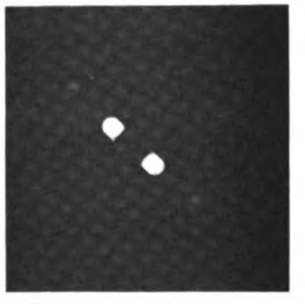

No. 2 45°


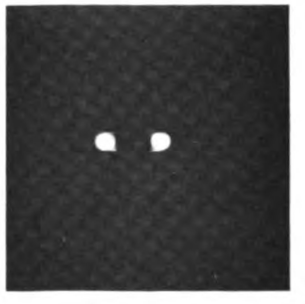

No. 3 90°


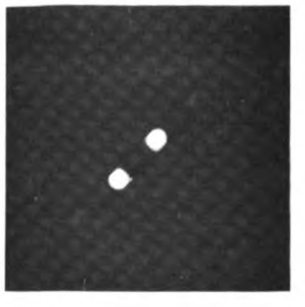

No. 4 135°

Fig. 4. The selective viewing of crossed gratings at various angles

Since Eq. (41) is a vector equation there is an angle θ associated with the vector $\bar{s}$ and the grating wave vector $\bar{k}^*$. The selective passing of crossed gratings at various angles by placing a slit at the same angle in the mask plane was the subject of a most famous study by Abbe[11] and is the essence of the concept of theta modulation[12]. As an example of theta modulation Fig. 4 shows four crossed gratings making up the numerals 1, 2, 3, and 4. Again the light distributions that are allowed to pass the mask plane are shown on the right and the final images are shown on the left.

B. Phase Contrast

The phase contrast method was developed by Zernike[13] in 1935. It has been a revolutionary tool in examining microscopic biological specimens which are often transparent but do introduce small phase shifts in the object function. Since the phase error $H(x,z)$ is small, the object function can be written as

$$E(x,z) = E_o \exp[iH(x,z)] \approx E_o [1 + iH(x,z)], \tag{42}$$

where E_o^2 is the intensity which is constant everywhere over the object plane. The light distribution approaching the mask plane is given by Eq. (10) as

$$E(u',w') = \frac{C}{f}\iint_B E_o \exp\left[-\frac{ik}{f}(u'x + w'z)\right] dx\, dz$$
$$+ \frac{C}{f}\iint_B E_o iH(x,z) \exp\left[\frac{ik}{f}(u'x + w'z)\right] dx dz \,. \tag{43}$$

The first term on the right of Eq. (43) gives an Airy pattern in the center of the mask plane. Since microscopic specimens usually contain high spatial frequencies, the second term on the right gives a distribution of light generally at some distance from the central area of the mask plane.

Placing a quarter wave plate over the central area introduces a masking function given by

$$M(u',w') = b \exp\left[-\frac{i\pi}{2}\right] = -ib, \tag{44}$$

which operates on the first integral to produce a $\pi/2$ phase retardation and a fractional reduction of amplitude , b^2 being the transmission of the phase plate. The mask function M(u',w') has little effect on the second integral if the spatial frequency of H(x,z) is sufficiently high to give negligible contribution in the central area. The light distribution leaving the mask plane then is

$$E'(u',w') = -\frac{C}{f}\iint_B E_o ib \exp\left[-\frac{ik}{f}(u'x + w'z)\right] dx dz$$
$$+ \frac{C}{f}\iint_B E_o iH(x,z) \exp\left[-\frac{ik}{f}(u'x + w'z)\right] dx\, dz \,. \tag{45}$$

With the redefined coordinates x'z', the second Fourier transform gives the image as being just the object but with the constant term multiplied by -ib. The image then is given by

$$E(x',z') = E_o i\,[-b + H(x,z)] \tag{46}$$

Now it can be seen from Eq. (43) that H(x,z) now adds in parallel in the image, not perpendicularly as in the object. This means that the intensity, which is the absolute value of Eq. (46), varies with the phase factor H(x',z') and is no longer a constant as in the object function Eq. (42). It can also be seen that the contrast can be controlled somewhat by varying b.

Examples of microphotographs are shown in Fig. 5 with and without the phase plate over the central area.

C. The Schlieren System

All systems used for visualization of phase objects by the use of opaque Fourier mask are termed schlieren systems[14]. There are many types due to various source-mask pairs and various configurations of lenses or mirrors. Three special cases will be treated here, the null schlieren, which has been used as a model Fourier mask system from the outset, the schlieren interferometer, and the case of isochromates.

1. The Null Schlieren System

As would be expected from the name, the null schlieren system is used for viewing very feeble phase objects. The mask of the null system just covers the source image in the mask plane. Let us begin by calculating the system's sensitivity for the case of a small circular source-mask pair of radius a. The insertion of an object will produce a displaced image in

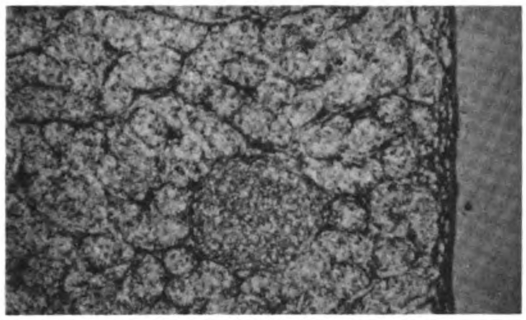

a. Testis 200X Phase Contrast

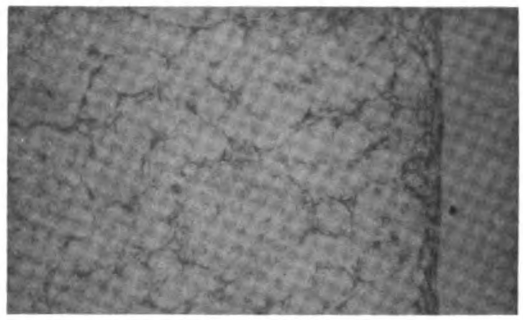

b. Testis 200X Bright Field

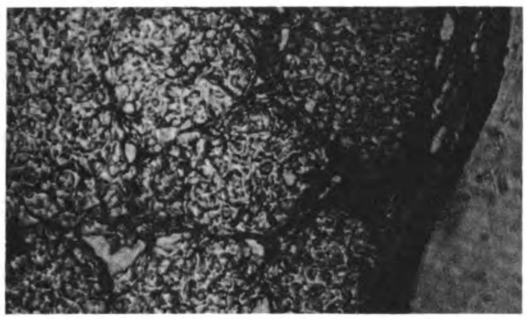

c. Testis 860X Phase Contrast

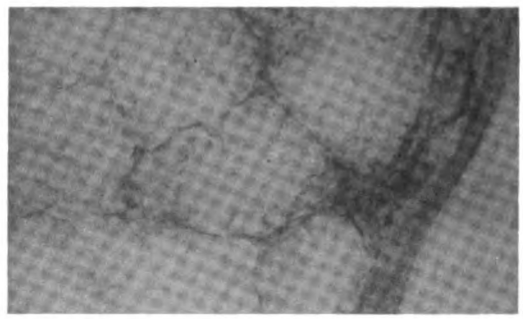

d. Testis 860X Bright Field

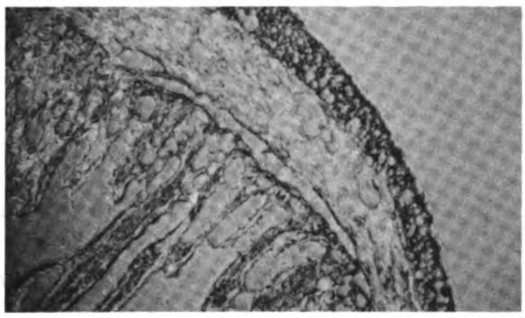

e. Intestine 200X Phase Contrast

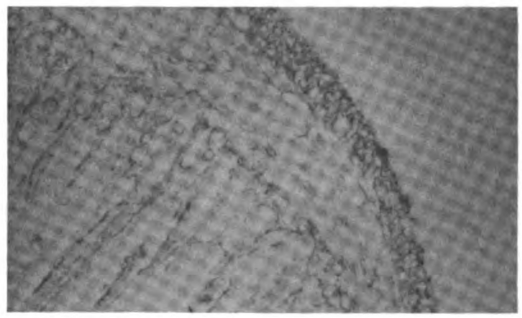

f. Intestine 200X Bright Field

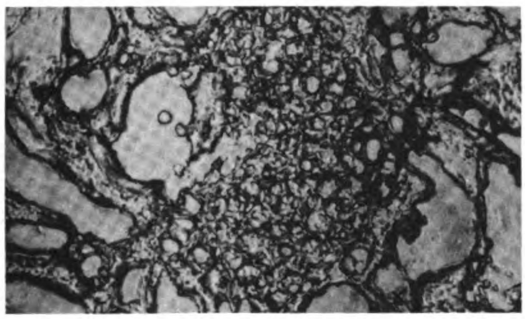

g. Kidney 860X Phase Contrast

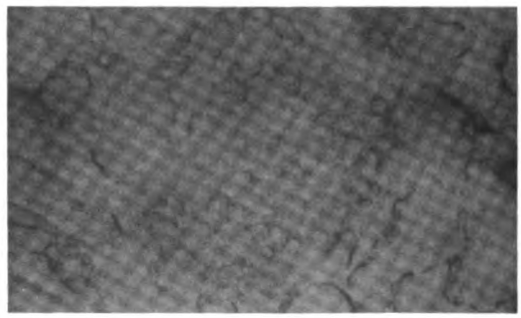

h. Kidney 860X Bright Field

Fig. 5. Examples of phase contrast microphotographs

the mask plane. The displacement d can be found from Chapter III for the various types of objects as

$$d = \frac{b_1}{k} f \qquad \text{refractive wedge} \tag{47}$$

$$d = \pm \frac{k^*}{k} f \qquad \text{sinusoidal amplitude grating} \tag{48}$$

$$d_n = n \frac{k^*}{k} f \qquad \text{sinusoidal phase grating} \tag{49}$$

where b_1 is defined in Eq. (21B) and d_n is the displacement of the n^{th} diffraction order for a phase grating. In the third case account must be taken of the amount of light in each order which is a function of the maximum phase shift V. In this case the average displacement of light can be written as

$$d = \frac{\int u' J_n(V)\, du'}{\int J_n(V)\, du'} \quad . \tag{50}$$

For a given displacement d the light in a circular image that will pass a circular obstacle of the same radius a can be found from geometrical considerations[15] as

$$S(d) = S_o \left\{ 1 - \frac{2}{\pi} \left[\arccos \frac{d}{2a} - \frac{d}{2a} \left(1 - \frac{d^2}{4a^2}\right)^{1/2} \right] \right\} \quad , \tag{51}$$

where S_o is the brightness of the displaced image or the average brightness in the case of a phase grating. If a vertical slit source and a line mask both of width 2a were used then S(d) would be given by

$$S(d) = \begin{cases} S_o \dfrac{d}{2a} & \text{for } d < 2a \\ S_o & \text{for } d > 2a. \end{cases} \tag{52}$$

These two cases are plotted in part a and b of Fig. 6.

The amount of light passing the mask can be increased by adding more small circles or lines, in the source and mask planes. This will multiply the right hand sides of Eq. (51) and (52) by the number of identical sources added. This only increases the speed of the system just as though one had used a brighter light bulb. It should be pointed out that the new sources and masks pass no new information to the final image. In addition we must now take into account the possibility that the displaced image of a particular source might be blocked by a nearby mask. This gives rise to curves like Fig. 6c which show the light passing through a Ronchi ruling source-mask pair as a function of the separation d.

Still another problem is encountered when multiple source-mask pairs are used. A very small object in the object plane B will diffract light uniformly over the mask plane. This coherent light passing through the various parts of the mask, especially if the mask shows any regularity, will tend to interfere beyond the mask and may cause multiple images. Figure 7a is a null schlieren photograph of a loaded plexiglas beam taken with a Ronchi ruling source-mask pair. This photograph very clearly shows the undesirable effect of multiple images.

The multiple images may be eliminated by randomizing the source-mask pair. This does not eliminate interference in the final image, but it does render the interference unrecognizable. The final image then appears as if there were just some loss of resolution. Figure 7b is a null schlieren photograph of the same loaded Plexiglas beam taken with the source-mask pair

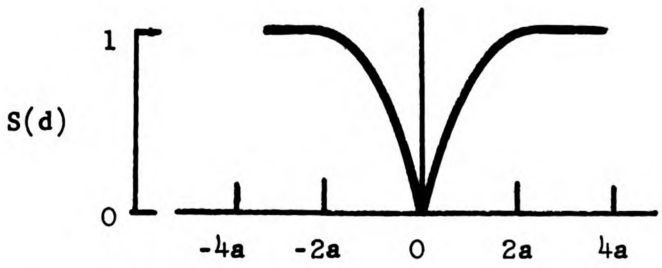

a. A point source and a dot mask

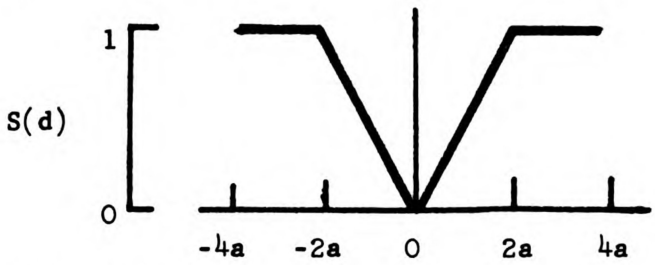

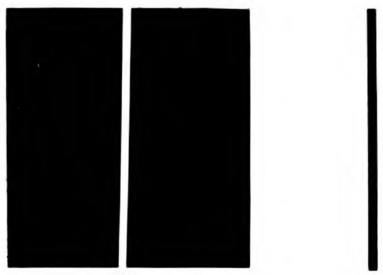

b. A slit source and a line mask

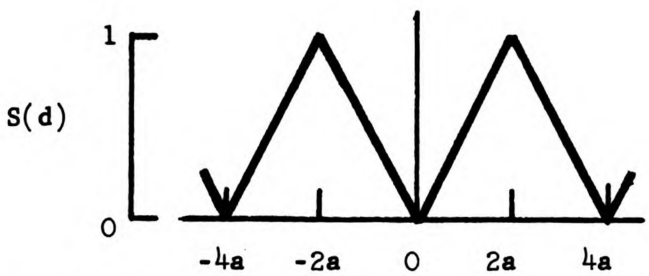

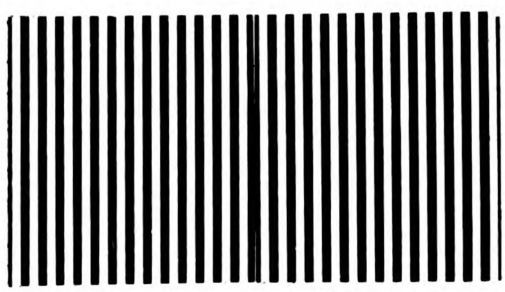

c. A Ronchi ruling source-mask pair

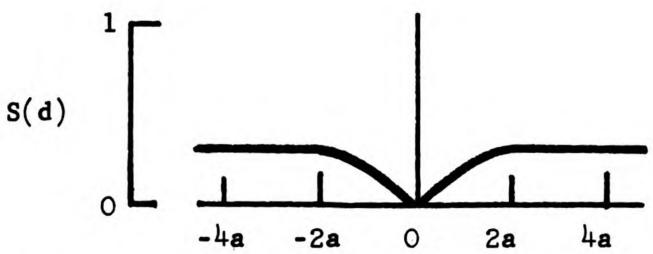

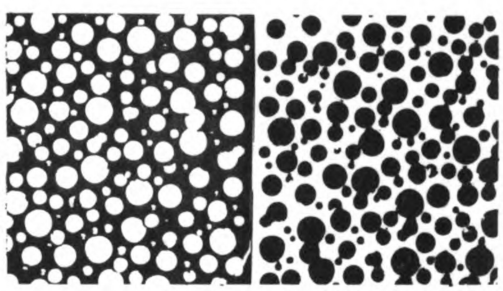

d. A random source-mask pair

Fig. 6. The spatial frequency responce of various source-mask pairs

shown in Fig. 6d. This photograph clearly shows only a single image, and some loss of resolution just as anticipated.

Figure 8 shows several null schlieren photographs taken with the source-mask pair shown in Fig. 6d. These photographs seem to be an improvement over those shown in earlier literature.

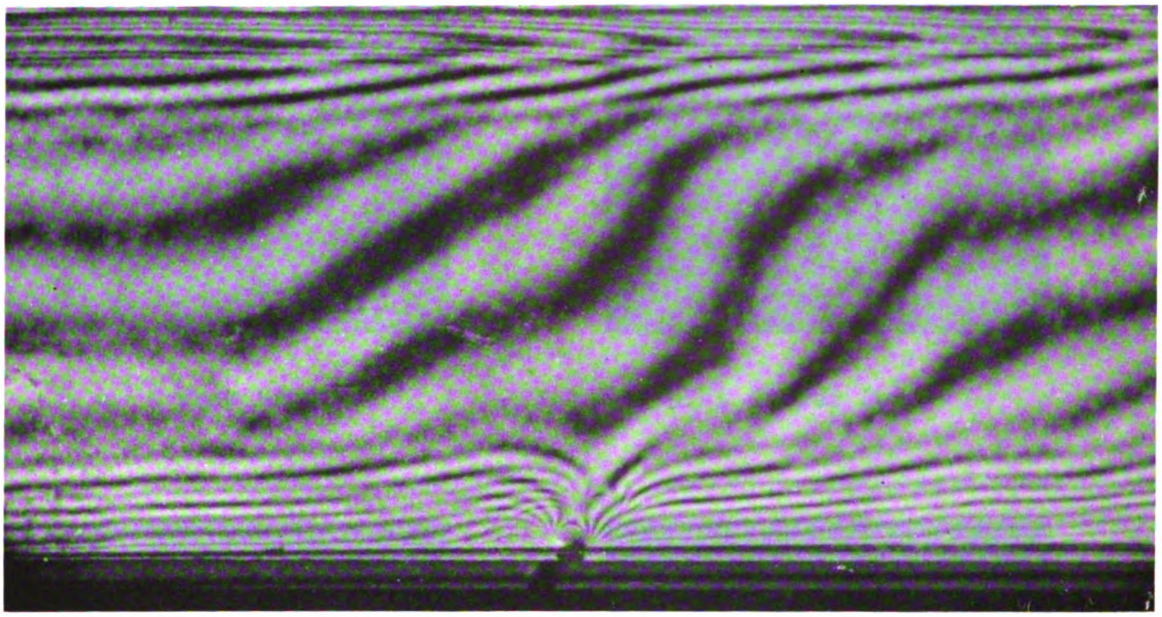

Regular Source-Mask Pair

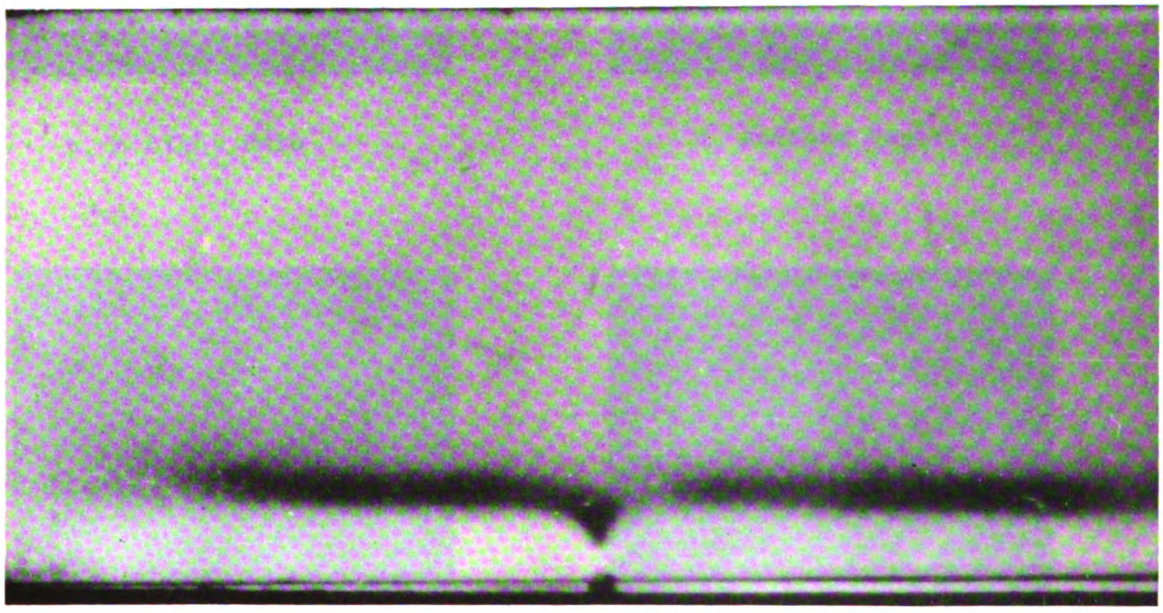

Random Source-Mask Pair

Fig. 7. The Effect of Regular or Random Source-Mask Pairs

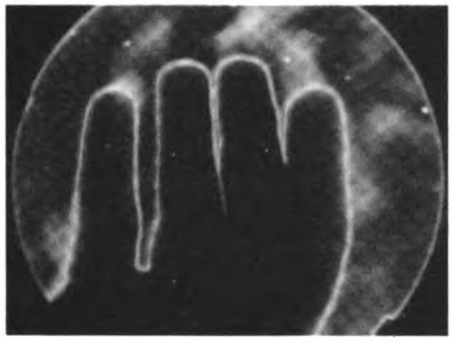

a. A Warm Hand

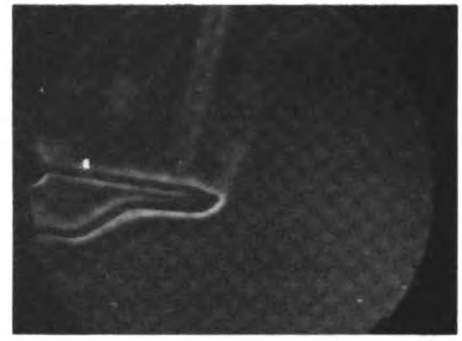

b. A Solder Gun

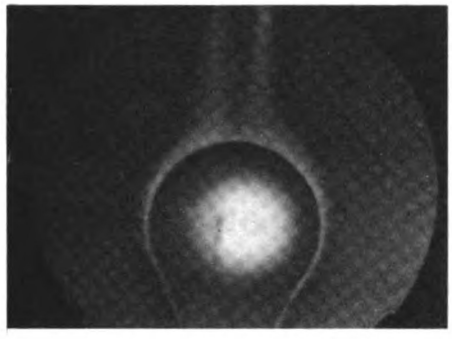

c. A Light Bulb

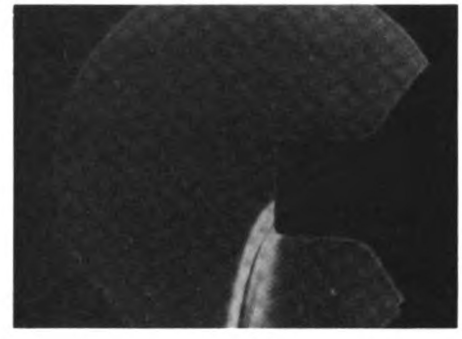

d. Acetone Vapor

e. A Burning Match

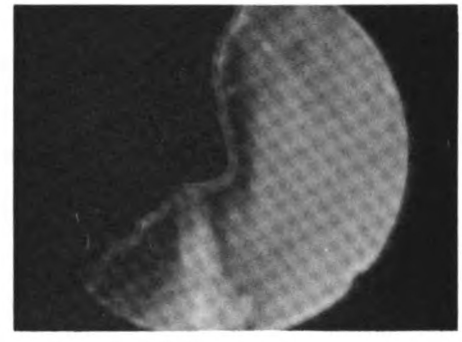

f. Warm Breath

Fig. 8. Sample Null-Schlieren Photographs

2. The Schlieren Interferometer

It has been found[16] that by placing an obstacle in the mask plane that is somewhat smaller than the image of the point source one can construct an interferometer which will produce photographs exactly like a Mach-Zehnder interferometer that is adjusted so that one fringe covers the entire field.

By way of an explanation the case of a thin glass wedge in the center of the object field will be treated for the one dimensional case. As shown in Fig. 9a the object function can be taken in two parts. The first E_1 is due to the area surrounding the glass wedge, and its Fourier transform in Fig. 9b is very similar to the Airy pattern for a full aperture. The Fourier transform of the light due to the wedge E_2 is just a displaced Airy pattern in the mask plane. A small obstacle is placed at the center of the axial Airy pattern in Fig. 9c. This has the effect of subtracting a delta function in Fig. 9d. The Fourier transform of each term is taken in Fig. 9e and these are added to obtain the final image as shown in Fig. 9f.

It can be seen from Fig. 9f that there will be a series of fringes in the central area. A bright fringe will appear at each interval given by

$$H(x,z) = (N + 1/2)\, 2\pi \tag{53}$$

just as with the Mach-Zehnder interferometer.

Several examples of schlieren interferometer photographs are shown in Fig. 10.

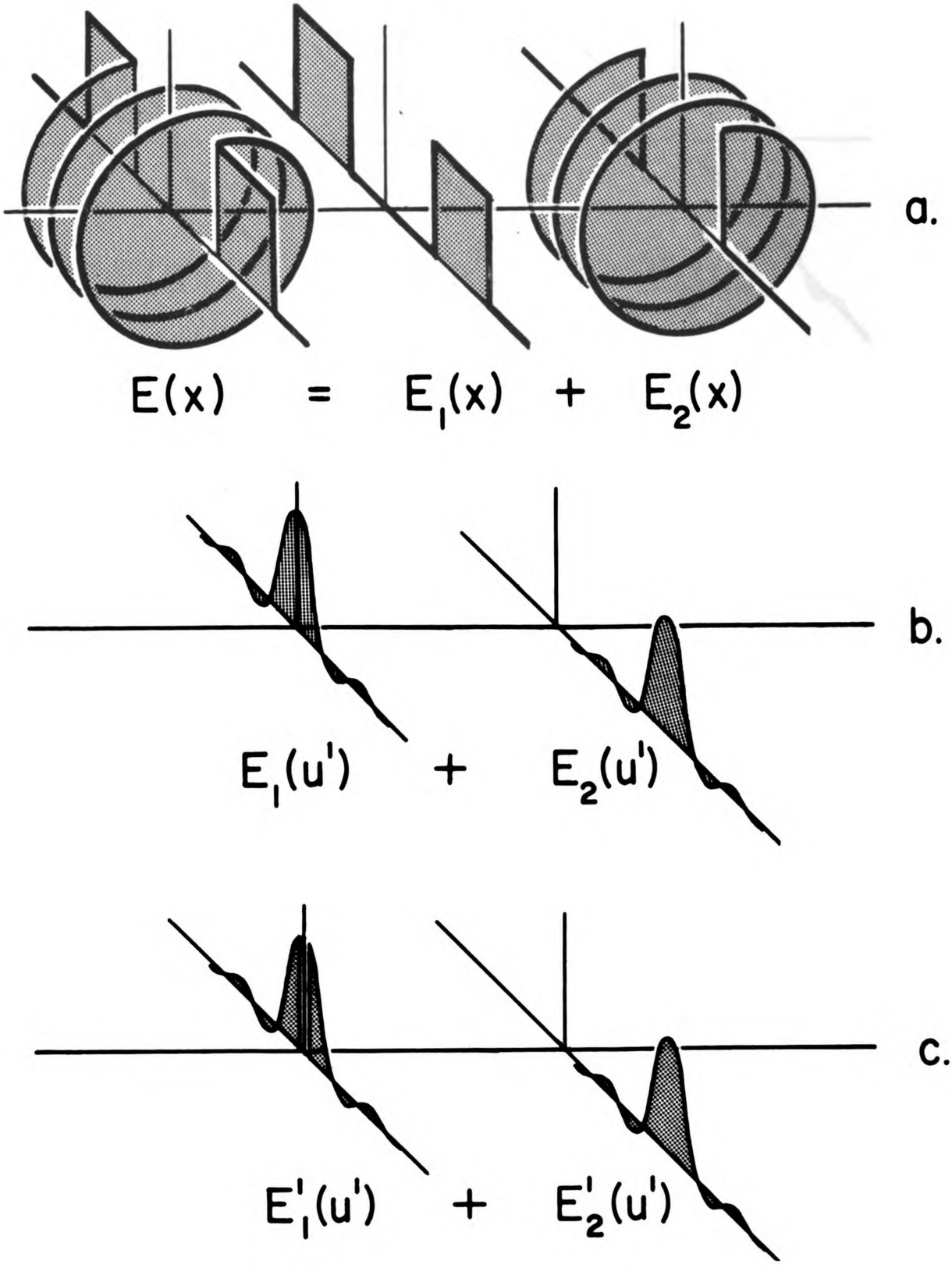

Fig. 9. Phasor Diagram of a Glass Wedge in a Schlieren Interferometer

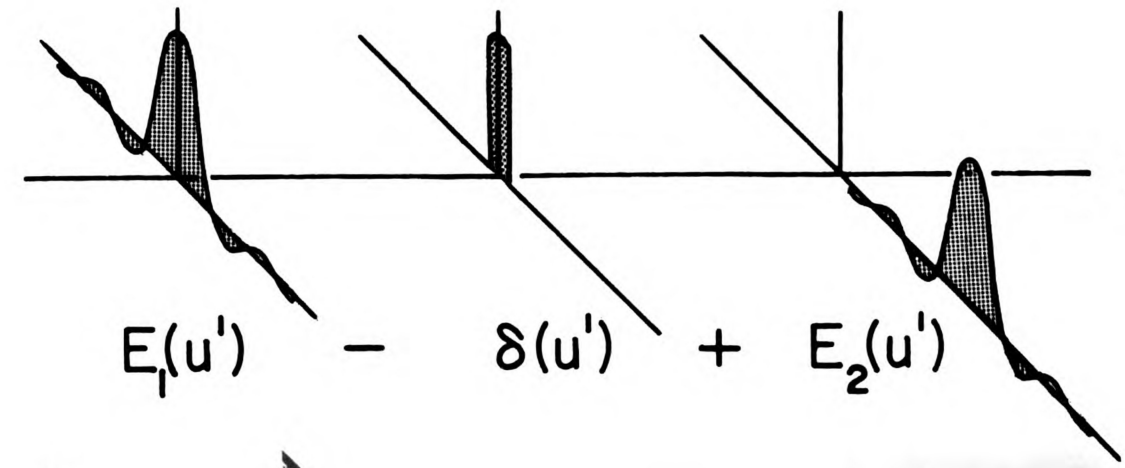

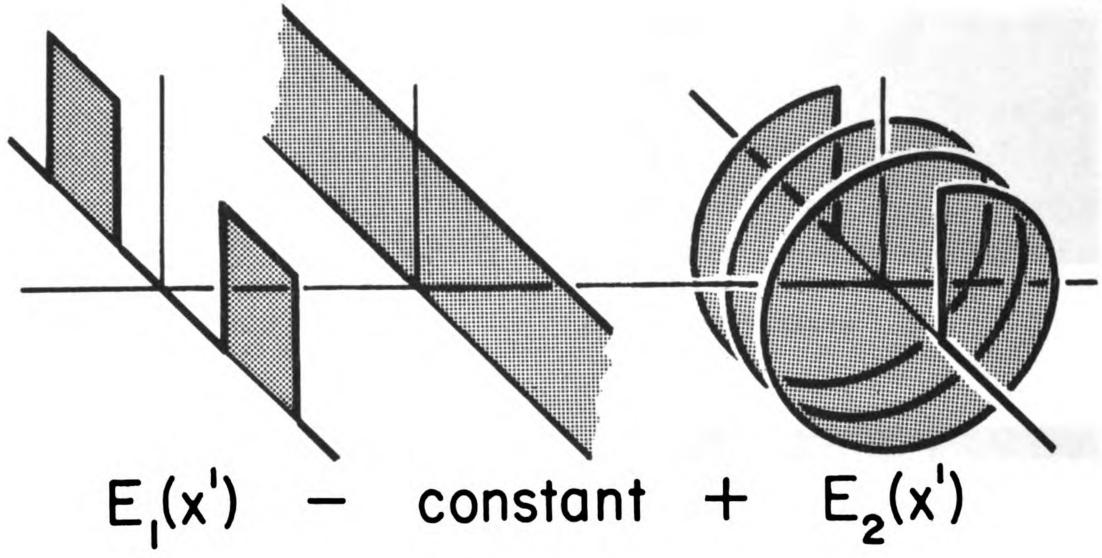

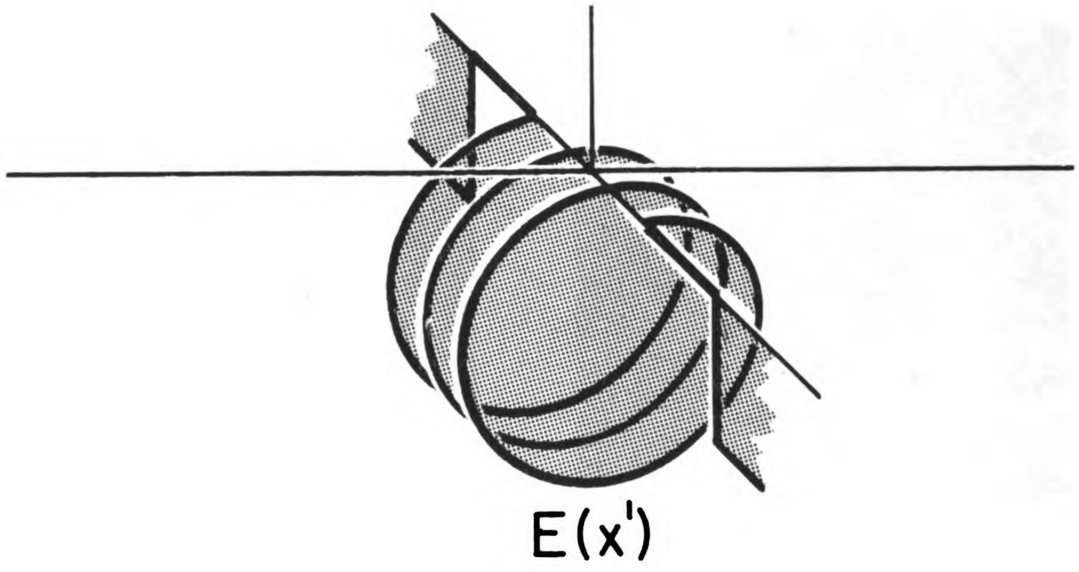

Fig. 9 con't.

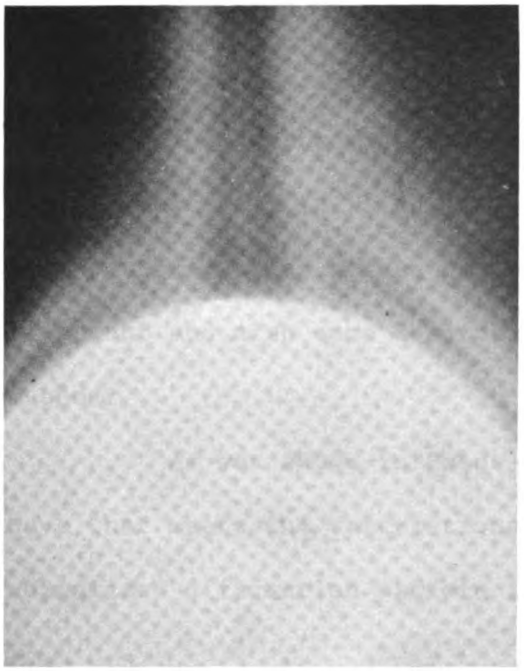

a. A Hot Light Bulb

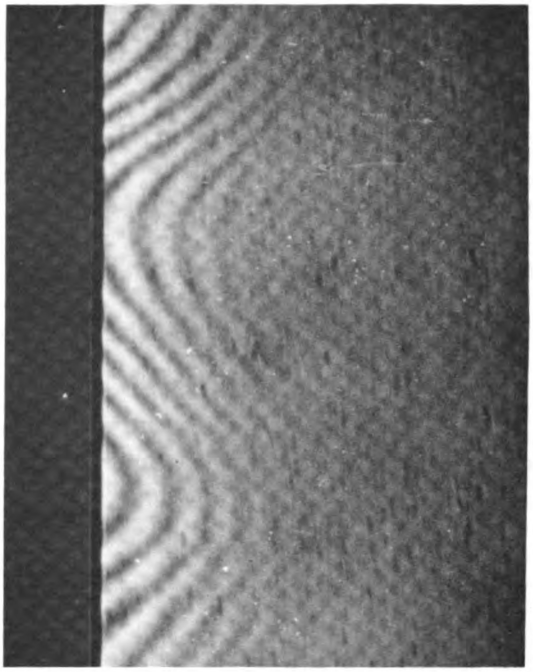

b. Ordinary Glass

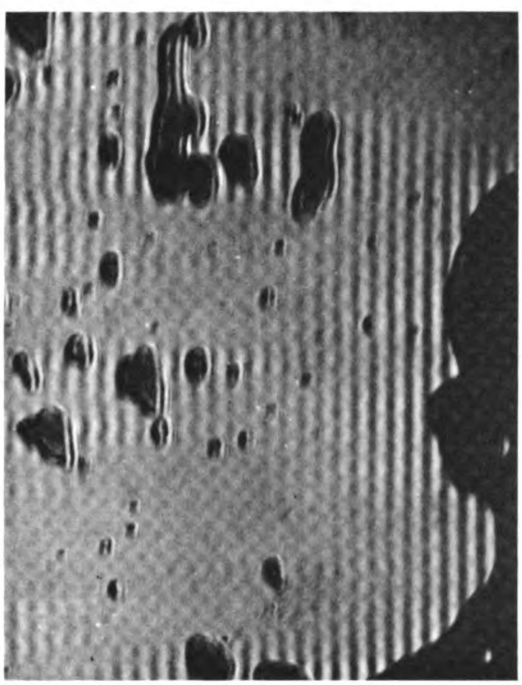

c. Water Between Two Flats

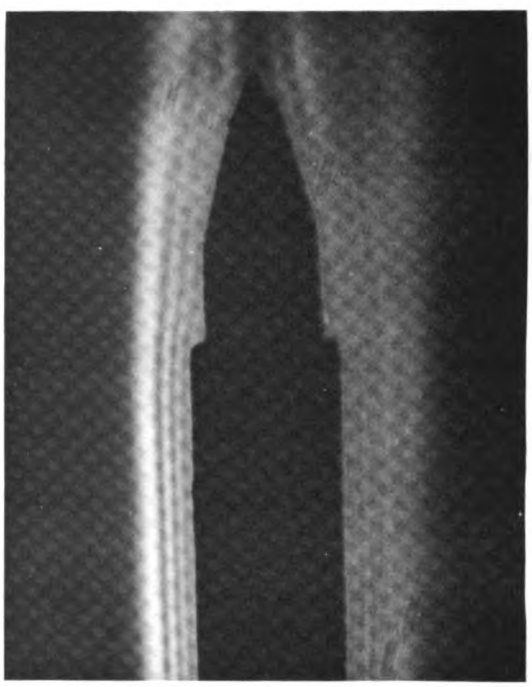

d. A Hot Solder Gun

Figure 10. Examples of Schlieren Interferometer Photographs

3. The Isochromate Effect

The isochromate effect was discovered in 1938 by Hiedemann and Osterhammel[17]. It is an interesting and beautiful way to view ultrasonic beam patterns. The method has been used to determine ultrasonic transducer alignment and also some absorption measurements have been made by this method.

As was shown in Chapter III, for a purely sinusoidal ultrasonic wave that meets the restrictions of behaving like a phase grating the normalized diffraction pattern in the mask plane is given by

$$I_n = J_n^2(V), \tag{54}$$

where the maximum phase shift V for an ultrasonic wave is given by

$$V = k\,(\mu_{max} - \mu_o)\,D. \tag{55}$$

Here $(\mu_{max} - \mu_o)\,D$ is the difference in optical path length through the undisturbed medium and through the most compressed part of the sound wave. To shorten the notation let us define $(\mu_{max} - \mu_o)\,D \equiv [D]$.

Now consider a mask that allows only the central diffraction order to pass. The light passing the mask is given by

$$I' = J_o^2\,(V)\ . \tag{56}$$

The intensity of the unobstructed central order is plotted verses the maximum optical path difference [D] for several colors of light in Fig. 11.

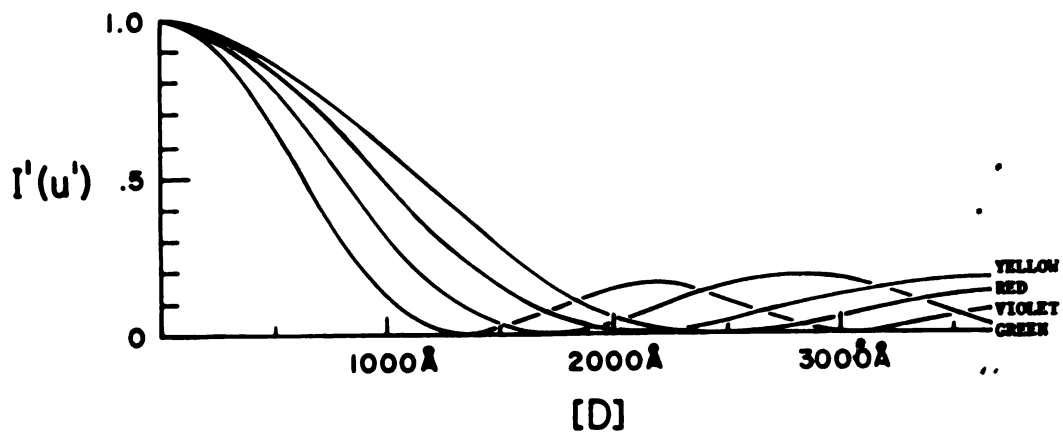

Figure 11. The Central Order of Light Diffracted by an Ultrasonic Wave.

It is seen that for a white light source and an optical path length difference of 1500Å, the zero order will be essentially red. Since the zero order is the only one that is allowed to pass, all parts of a sound field that have D = 1500Å will appear red and all parts of the sound field that have D = 2100Å will appear blue, hence the name isochromate. Since all of the Bessel function pass through zeroes, similar pictures can be made by passing any order.

Some examples of isochromate photographs of various ultrasonic beam patterns are shown in Fig. 12.

Figure 12. Isochromate Photographs of Various Ultrasonic Beam Patterns

VI. CONCLUSION

Throughout this paper an attempt has been made to choose terminology and mathematical expressions that are directly associated with the physical situation. For instance, if the usual procedure of optical mathematics had been followed, the final image distribution given by

$$E(x'z') = \frac{C}{R_2}\iint_{A'} M(u',w')\ E(u',w')\ \exp\left[-\frac{ik}{R_2}\ (u'x+w'z')\right]du'dw', \tag{57}$$

would have been expressed by way of the convolution theorem in terms of the Fourier transforms of M(u',w') and E(u',w'). This would be a much neater form but it fails to give any physical meaning to how the mask affects various information from the object. Hence, a mathematical procedure has been advanced rather than a single expression. This procedure has given considerable insight into the operation of Fourier mask systems, and has in the case of many of the photographs shown, led to the optimum configuration of sources, lenses, and mask for the particular object in question.

VII. BIBLIOGRAPHY

1. A. B. Porter, Phil. Mag., 11, 154 (1906).
2. G. G. Stokes, Trans. Camb. Phil. Soc., 9, 1 (1849).
3. G. N. Watson, A Treatise on the Theory of Bessel Functions (Cambridge University Press 1922), p.20.
4. M. Born and E. Wolf. Principles of Optics (Pergomon Press 1959), p. 111.
5. E. B. Temple, J. Opt. Soc. Am., 47, 91 (1957).
6. E. Lommel, Abh. Bayer. Aked., 15, 233 (1885).
7. A. Marechal and P. Croce, Compt. Rend., 237, 706 (1953).
8. E. L. O'Neill, I.R.E. Trans. - P.G.I.T., 2, 56 (1956).
9. L. E. Hargrove, Private Communication.
10. C. V. Raman and N. S. N. Nath, Proc. Indian Acad. Sci. 2 406 (1935).
11. E. Abbe, Archiv. f. Mikruskopische Anat., 9, 413 (1873).
12. J. D. Armitage and A. W. Lohman, Appl. Opt., 4, 399 (1965).
13. F. Zernike, Z. Tech. Phys., 16, 454 (1935).
14. A. Toepler, Pogg. Amn., 134, 194 (1868).
15. M. Francon, Modern Applications of Physical Optics, (John Wiley and Sons 1963), p. 64.
16. E. L. Gayhart and R. Prescott, J. Opt. Soc. Am. 39, 540 (1949).
17. E. Hiedemann and K. Osterhammel, Proc. Indian Acad. Sci., 8, 275 (1938).